JETIR.ORG ISSN: 2349-5162 | ESTD Year : 2014 | Monthly Issue
JOURNAL OF EMERGING TECHNOLOGIES AND INNOVATIVE RESEARCH (JETIR)
An International Scholarly Open Access, Peer-reviewed, Refereed Journal

ELECTRIC VEHICLES TO SMART GRIDS ACTIVE AND REACTIVE POWER CONTROL STRATEGIES BY FUZZY CONTROLLER

[1]J LATHA, [2]Dr.G. JAYA KRISHNA

[1]PG scholar in Holy Mary Institute of Technology & Science, Bogaram (V), Medchal District, Hyderabad, India in the Dept. of Electrical & Electronics Engineering.

[2] Professor in Holy Mary Institute of Technology & Science, Bogaram (V), Medchal District, Hyderabad, India in the Dept. of Electrical & Electronics Engineering.

Abstract: Electric vehicles (EVs) can be used as distributed energy storage devices to provide to the smart grid different regulation services. However, to have enough impact on the grid, the trend is to jointly manage a set of EVs by means of a new stakeholder called an aggregator. Knowing the availability, mobility habits, and state of charge (SOC) of each EV battery, the aggregator performs the allocation of an active and/or reactive set-point to each EV within a time slot. This paper aims to propose reference charger currents for each EV from the individual set-point received by an aggregator. Control strategies for bidirectional active power control are compared under ideal and distorted source conditions. The control of the individual electric vehicle charging processes is decentralized, while a separate central control deals with the power transfer from the AC grid to the DC bus. The electric power exchange does not rely on communication links between the station and vehicles, and a smooth transition to vehicle-to-grid mode is also possible. The GSS has multiple Discharging Units (DUs), which transfer active and reactive power from EVs' batteries to the grid. In this paper, a fuzzy-based control method is developed for EVs which regulates the active and reactive power for grid support. The active and reactive power flow from GSS to the grid is based on the node voltage and amount of energy available in the GSS. Simulations are performed in Matlab/Simulink to illustrate the behavior of the station. The results show the feasibility of the model proposed and the capability of the control system for fast DC charging and also vehicle-to-grid.

I. INTRODUCTION

Charging time reduction is one of the key goals in making electric vehicles user-friendly. In this context, fast DC charging offers an interesting opportunity. It allows for reducing charging times to ranges of 10 to 20 minutes [1]. All levels use off-board electric vehicle supply equipment (EVSE). In this paper, modeling and simulation of an electric vehicle charging station for fast DC charging are proposed and formulated in an educational way in order to allow its implementation and further research on the topic.

Rising concern about pollution in cities along with the great advance in battery research has caused the commercial launch of electric vehicles (EV). They constitute an emerging industry that is expected to increase in the future. In this context, the energy stored in vehicles' batteries could be used to provide some services to the grid in their idle time. Depending on the power flow direction, two kinds of tasks can be distinguished: unidirectional, when EVs only charge their batteries with a strategy compatible with Demand Side Management (DSM) programs (usually known as grid-to-vehicle, (G2V) mode), and bidirectional, if batteries in EVs can also discharge to accomplish regulation services to the grid, concept known as vehicle-to-grid (V2G) mode [1]. Among the different regulation services that EVs can provide the grid with, Demand Side Management, smoothing of renewable energy resources (RES) injection of energy, and opportunity for providing ancillary services are worth mentioning [2]. The first one can be addressed by means of a scheduled charging plan according to economic aspects as well as grid requirements. Regarding the smoothing of RES injection, the "shiftable" character of this kind of load allows moving the charging period to the hours with high RES production, so contributing to pollution reduction and reducing charging costs. Unlike these mentioned tasks, ancillary service providing requires bidirectional power flow, thus adding technical constraints as well as economic opportunities to EV owners. For the above-mentioned services to have enough impact in the grid, and with the aim of overcoming the limitation of capacity, availability, and durability of individual batteries, an aggregation is required. The trend is to jointly manage a fleet or a set of EVs by means of a new stakeholder called an aggregator. The main role of the aggregator is to optimize an objective function (to maximize revenues, to minimize costs or to prioritize consumption of energy coming from RES), subjected to constraints relative to availability of EVs, mobility habits,

SOC and degradation of batteries [3]. Many papers can be found in the literature that deal with algorithms to allocate active power set-points among the EVs under the aggregator management [1, 3-5], with the main objective to participate in active power control reserve services. The definition of the objective function to optimize, the treatment of constraints are assessed in most of them. However, scarce references are found about the possibility of contribute to reactive power support and even voltage control in the bus where a set of EVs are connected [2, 6]. Regarding incentives to motivate EV owner to participate in regulation services, there may consist of providing them with some attractive services in compensation or designing a different-price scheme for charging/discharging, even depending on the battery SOC. According to the kind of incentive selected, two types of control can be defined [7]:

Direct control implies that a service provider can order the charging/discharging rate of the EV batteries connected in a certain time period directly. The advantages of such direct control are prompt and predictable reactions to control signals. However this kind of control could cause rejection from the EV owners, since mobility is their primary purpose of use. It is more suitable for short-term control [3].

Indirect control consists of sending price signals to EV owners for them to decide to either reduce or shift the charging load when the price is high, or pay the higher price. This control is meaningful when EV owner is considered as a consumer and the objective is to apply a Demand Side Management strategy, but it is being studied for discharging prices as well. Disadvantages arise from the necessity to predict the reaction of owners to different price signals. Long-term control may be performed with this tool. In any case, the result of an optimization process to decide the contribution of each individual EV of an aggrupation to provide a regulation service, is the allocation of an active and/or reactive set-point to each battery within a time slot.

II. BATTERY CELLS AND TRACTION DRIVES

BMSs for battery cells and converter topologies available in the technical literature. The comparison among the BMSs has been carried out according to the complexity of the circuit design, balancing speed, voltage/current stress across the devices, balancing system efficiency, size and cost. The comparison between traction drive topologies has been carried out in terms of the complexity of the converter design and control system, harmonic content of output voltages and currents, blocking voltage of each semiconductor switch, switching losses, and fault tolerant capabilities.

Battery Management Systems Series connection of battery cells are widely used to reach the voltage required by the dclink of battery EV traction inverter [8]. However, voltage imbalance between the cells appears when the battery is charged or discharged several times, because of the differences in leakage currents, temperatures, internal impedances, charge storage volumes and chemical characteristics of the cells themselves. The voltage imbalance results in progressive damage of battery cells and reduction of their service life time [9]. In order to avoid this, BMSs are normally added to the battery pack [10]. One of the most important parameter that is required by the BMS is the SOC of the cells, which is a good indicator of the current state of the battery. A tight equalisation of the SOC across the cells minimises the damage to the cells [11]. There are two categories of charge equalising techniques used in BMS: passive BMSs and active BMSs. Passive BMSs use external passive resistors to dissipate the excess energy from the cells at higher SOC until their SOCs match those of at lower SOC. The resistors used in passive BMS can be either fixed in value [12], [13] or switched [12], [14]-[18], [19]-[21]. Active BMSs transfer the excess energy from the cells at higher SOC to the cells at lower SOC. Active BMSs topologies use different active elements as a buffer to transfer the energy between the cells, i.e. capacitors, inductors or transformers, as well as different controlled switches or converters [12], [14]-[18] and [21]-[46]. Passive BMSs are cheap and simple to implement with a reduced number of extra components. However, the equalisation rate is slow and the efficiency is low, because all the excess energy is dissipated across the balancing resistors. On the other hand, active BMSs provide a faster balancing rate and a higher efficiency, although they have higher complexity and cost [47]. The next sections provide a review of the different proposed passive and active BMSs [12]-[46], including their operating principle and the advantages and disadvantages of each method.

Converter-based BMSs Converter-based BMSs use power converters to balancing the cells or group of cells in a battery. These methods can be divided into Ćuk converters (CC), buck/boost converters (BBC), flyback converters (FbC), quasi-resonant converters (QRC), ramp converters (RC), and fullbridge converters (FBC). They feature a fully controlled balancing process, but the resulting BMS has relatively high cost and complexity [36]-[44].

III. Ćuk converters

The circuit diagram of the bi-directional CC balancing system. This method uses N − 1 bi-directional Ćuk converters to balance a series string of N battery cells; each converter consists of two switches, two inductors and one capacitor. Each converter is connected across two adjacent cells to allow the energy transfer from the cell with a higher voltage to the cell with a lower voltage. Therefore, this method takes a relatively long time to equalise the entire pack, especially for a high number of cells. The maximum voltage across each switch is equal to the maximum capacitive voltage (VB1 + VB2) and, hence, low voltage MosFETs can be used as power devices to reduce conduction and switching losses [36], [37].

The energy is transferred between two adjacent cells through the capacitor, where the direction of the power is determined by the voltage imbalance between the two cells and the switching function of the switches. The converter is usually designed to operate in discontinuous capacitor voltage mode (DCVM) in order to reduce MosFETs switching losses. The initial voltage across the capacitor is equal to the voltage sum of the two adjacent cells [36], [37]. This method can achieve cell balancing with high efficiency, so it is suitable for both EV and HEV applications, but the speed of cell balancing is slow and the control system is complex [36], [37].

IV. BUCK/BOOST CONVERTER

The buck, boost, and buck-boost converters are commonly used as active BMSs. Buck converters are used to transfer the energy from the battery pack to the cells at lower voltage;

boost converters are used to transfer the excess energy from the cells at higher voltage to the battery pack; and buck-boost converters can be used in either direction. The BBC methods can achieve a good equalisation speed with high efficiency and they are suitable for modular design. On the other hand, the implementation is relatively expensive and complex and a complex control is needed to achieve cell balancing [14]-

[16], [38], [39]. Fig. 2.14 shows the circuit diagram of the buck/boost conversion balancing system. This method uses N bidirectional SMs to balance the series string of N battery cells. Each SM consists of two switches, one inductor and one capacitor. The converters can be operated in continuous conduction mode (CCM) or discontinuous conduction mode (DCM), depending on the design of the control and the circuit parameters. The maximum voltage of each SM is equal to the cell voltage and, hence, low voltage MosFETs can be used also in this case [14]-[16], [38], [39]. During the charging process, each SM operates as a buck converter. Therefore, the capacitors of the output filters are connected first in series, and then to the dc power source. The balancing system operates without filter capacitor at the SM input terminals [14]-[16], [38], [39]. During the discharge process, the SMs draw currents from cells to increase the voltage of the output capacitors and then the sum of the output voltages of SMs is controlled to meet the required load voltage. The average input/output voltage of each SM depends on the corresponding cell voltage and the SM duty cycle. Therefore, the average input/output voltage of the SMs may be different. However, the average input/output current of the SM is equal to the input charge current or to the output load current, because all SMs are connected in series and either charged by the same dc power source or discharged to the same load [14]-[16], [38], [39].

For CCM, the battery current can be regulated individually by adjusting the duty cycles of the converters. The cell current is inversely proportional to the duty cycles of the corresponding SM. For DCM, the module with higher voltage has the smaller time ratio of the switching period when the inductor current decreases from the peak value to zero, revealing that cell balancing can be automatically achieved when all SMs are operated with the same duty cycle

V. CHARGING STATION DESIGN

A variety of aspects needs to be taken into account when designing the circuit of the charging station. These aspects, from a technical point of view, include the following:

Area made available for parking of vehicles; this influences the number of cars that can be placed and charged.

Estimation of the demand for fast charging slots in the location.

Network parameters, i.e. nominal voltage and allowable power levels at the point of common coupling (PCC).

Maximum charging power rate for individual vehicles. The proposed DC charging station configuration is shown in Fig. 1, it can be seen that the inverter is interfaced to the network through an LCL filter and a transformer; while a single DC bus feeds all individuals battery chargers. The charging station rated capacity Srated in VAr is defined according to (1):

$$S_{\text{rated}} = \frac{k_{\text{load}} N_{\text{slot}} P_{\text{EV}}}{\cos\phi}$$

where cos φ is the power factor, Nslot is the amount of charging slots available for individual EVs, PEV is the maximal power rate of an individual EV and kload is an overload factor for cover overloading in transients. Generally, the DC link voltage is set according to the grid voltage. In this work, the grid connection through a transformer leaves the DC bus voltage selection free from the grid voltage level. However, it has to be considered that the battery minimum voltage V min bat , and the battery charger minimum modulation index mmin, define an upper bound for the DC bus voltage as in (2):

$$v_{\text{dc}} \leq \frac{V_{\text{bat}}^{\text{min}}}{m_{\text{min}}}$$

where vdc is the DC bus nominal voltage.

A. DC bus capacitance calculation

The stability of the DC bus depends directly on the DC capacitance size. Basically, it has to support the DC current ripple. As many EV chargers can be connected to the DC bus, ripple current can be very high needing for a huge capacitance. A good method to define the capacitance of a DC bus, including the resistance and the inductance of the cable is reported in [2]. Additionally, a practical method is reported in [3]. In this work, both methods are taken into account, and the DC capacitance is determined by the capacitor energy rate of change during transients and the rated active power. The calculation is proposed in (3):

$$C_{\text{dc}} = \frac{S_{\text{rated}}}{V_{\text{dc}}^2} \frac{2nT\Delta r \cos\phi}{\Delta x}$$

where T is the period of the AC voltage waveform, n is a multiple of T, Δr is the DC power range of change, in percent, during transients, and Δx is the allowable DC bus voltage range of change, in percent, during transients.

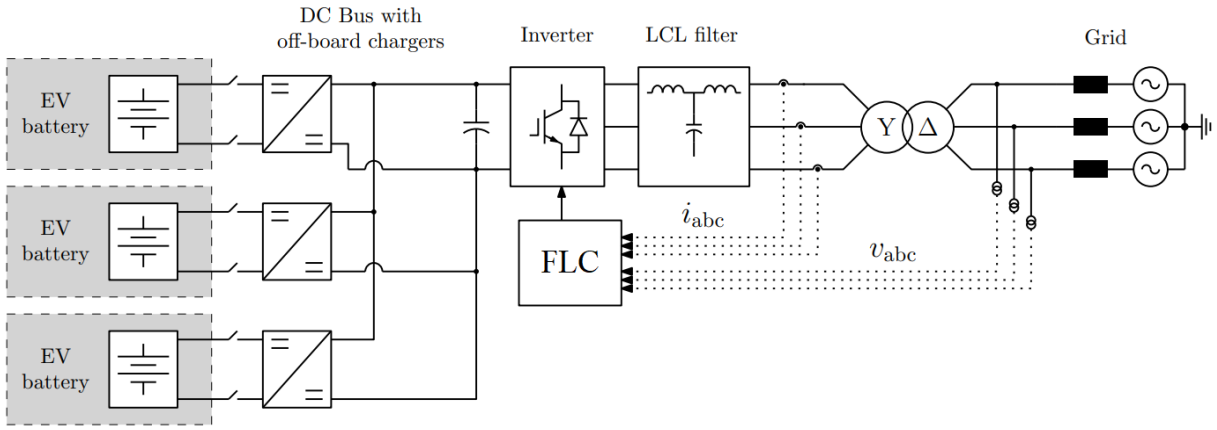

Fig. 1. Proposed EV charging station for fast DC charging.

B. EV battery

Nowadays, run time based models combined with Thevenin ´ equivalent based models are the state of the art [4]. In this work, such an approach is used. Fig. 2 shows the electric circuit configuration of the battery model. Here Voc is the open circuit voltage which is depending of the state of charge SOC, and the voltage-current characteristic is modeled by a series resistance Rseries. The RC parallel circuit represents the transient response of the battery.

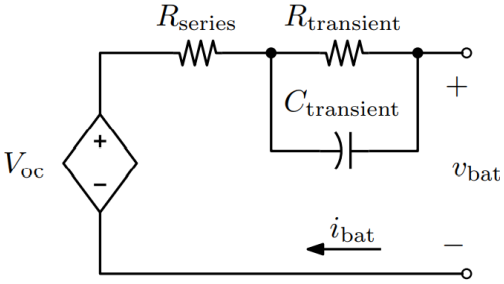

Fig. 2. Thevenin battery model.

Battery charger

Fig. 3 shows the modeled battery charger. It consists of a bi-directional DC-DC converter with two IGBT switches that are operated always by complimentary control signals [5]. This allows a continuous bi-directional power capability. When the lower switch is operating, the converter boosts the left-side voltage vbat, and the current ibat in the inductor Lbat flows to the capacitor C. When the upper switch is operating, the converter acts as buck-type converter, and ibat flows from capacitor C to the inductor obtaining an opposite direction of ibat.

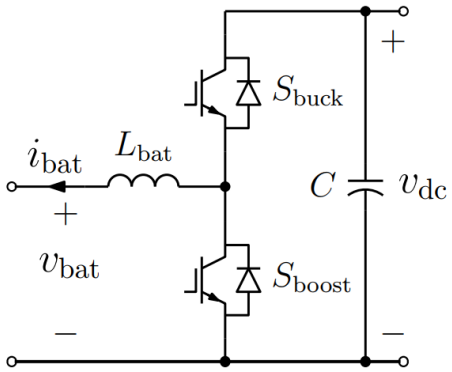

Fig. 3. Battery charger configuration.

C. Three-phase inverter

In this work for an educational purpose and simplicity of modeling, the inverter configuration is chosen as in Fig. 4. Here, the inverter is connected to an LCL filter.

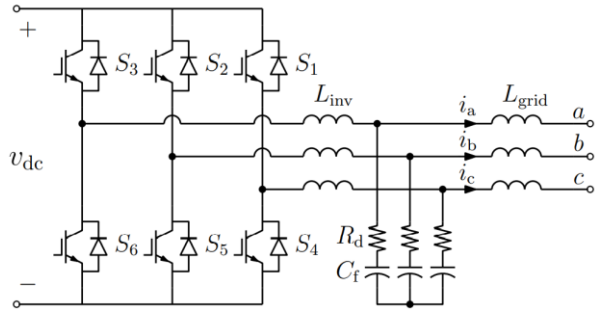

Fig. 4. Three-phase inverter plus LCL filter.

D. LCL filter

Passive LCL filters become as state of the art in harmonic reduction of grid-interfaced distributed power sources [6]. Different methodologies to determine the filter parameters can be found in the literature [7]–[9]. On the one hand, the selection of the inverter side inductance is based on DC voltage, inverter modulation index, switching frequency and current total harmonic distortion

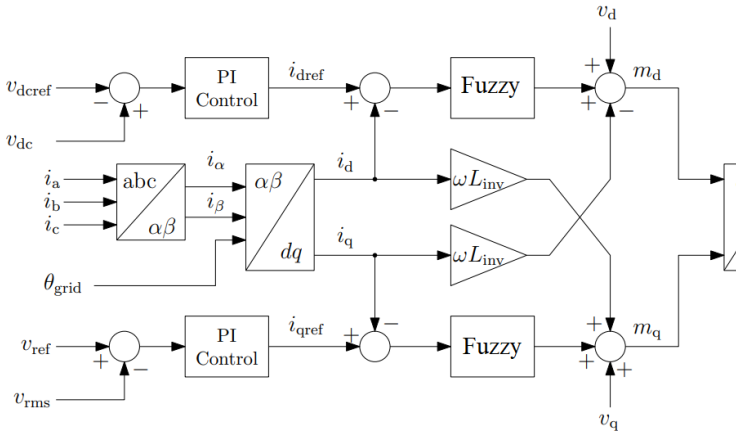

Fig. 5. Charging station control system.

THD. On the other hand, the selection of capacitance, and grid-side inductance depends on the grid parameters, reactive power, resonance frequency, and ripple attenuation factor (RAF) [7]. Fig. 4 shows the LCL filter configuration where the inverter-side inductance Linv, filter capacitance Cf and grid side inductance Lgrid are determined as in (4), (5), (6) respectively:

$$L_{inv} = \frac{V_{grid}^2}{S_{rated} \cdot THD \cdot 2\pi f_{sw}} \sqrt{\frac{\pi^2}{18}\left(\frac{3}{2} - \frac{4\sqrt{3}}{\pi} m_a + \frac{9}{8} m_a^2\right)}$$

$$C_f \leq \frac{0.05 S_{rated}}{2\pi \cdot f_{grid} \cdot V_{grid}^2}$$

$$L_{grid} = \frac{RAF + 1}{RAF \cdot C_f \cdot 2\pi f_{sw}^2}$$

In the previous equations, fsw is the switching frequency of the inverter, fgrid is the grid voltage fundamental frequency, ma is the inverter modulation index. THD is normally set between 5% and 30% [8] and RAF normally around 20% [7]. After obtaining the filter parameters, it should be verifiable that resonance frequency, defined in (7), should be in the range of less than half of the fsw and 10 times bigger than the grid frequency [7].

$$\omega_{res} = \sqrt{\frac{L_{inv} + L_{grid}}{L_{grid} L_{inv} C_f}}$$

If the resultant parameters do not match this condition, determination of Cf , range of T HD and range of RAF gives flexibility to match this condition. Finally, a damping resistor Rd is included as shown in Fig. 4 and it is calculated as in (8):

$$R_d = \frac{1}{3 C_f \omega_{res}}$$

VI. REACTIVE POWER MANAGEMENT IN SMART GRIDS

The traditional operation of distribution network does not allow the evolution of these networks. A new paradigm is required to include large quantities of distributed energy resources. The concept of smart grids covers a set of evolution in all voltage levels of power systems. The distribution network operation, the energy management, the resource management and the reactive power management are some of important topics in the smart grids analysis. A. Energy Resources Management in smart grids To manage the distributed resources, an energy resources management simulation tool called ERMaS was developed by the authors of this paper. In the scope of ERMaS, it is assumed that a VPP is able to operate different distributed energy resources in a specific network area [7]. The VPP must respect the contracts established with the available distributed resources, in order to achieve a good energy resource management solution. The ERMaS tool uses historical data and daily forecasted data to support the energy resource management process. These data concern the identification of the different DER that may be available in the network. The data base contains the forecasted values for each hour, regarding the day-ahead periods of forecasted consumption and forecasted generation based on natural resources (wind and sun). On the other hand, the information concerning the distributed generation capacity, storage status, available demand response events and network configuration is also necessary. The ERMaS includes deterministic and heuristic techniques to solve the energy resources management problem [7, 8]. The user can choose the deterministic technique if it is necessary an exact result or a heuristic technique (Particle Swarm Optimization, Simulated annealing or Genetic Algorithm), or if the user needs results in a short period of time [8]. The heuristic techniques have been implemented in Matrix Laboratory (MATLAB) [9] software, and the deterministic technique, mixed-integer non-linear programming (MINLP) has been modeled in General Algebraic Modeling System (GAMS) [10] software. MATLAB has also been used as interface with GAMS. In this way, GAMS is only responsible for modeling the deterministic technique, and MATLAB organizes the input data and receives the output data, and organizes the results in graphs. The main component of the ERMaS tool is the algorithm used to determine the energy resources management. The energy resources management is determined for different periods until it reaches the maximum number of envisaged periods (T). Typically, the energy resource management is executed for a period of 24 hours of the next day [8]. The energy resource management can be performed, in the scope of the ERMaS tool, using deterministic and metaheuristics techniques [8]. B. Reactive Power Management proposed methodologies Several energy resources scheduling methodologies only consider the management of active power in the medium and low voltage. However, it is important to consider the management of reactive power to improve the quantity of their resources connected to the distribution network and to optimize the operation reducing losses and the operation cost. The objective function represents the VPP's objectives, which present a mathematical significance. The VPP must be able to obtain a minimum cost or a maximum profit through a mathematical representation (objective function) of the involved objectives. In terms of the optimal resource scheduling, the most common approach is to develop an objective function that makes possible to maximize its profits.

Maximize f= $\forall t \in \{1,..,T\}$

However, to validate the effects and the impact of reactive power control, other objective function is proposed, considering the minimization of differences of the bus voltage magnitude. The inclusion of demand response variables in the objective function is important to avoid the cut of power demand when it is not necessary. If the term of demand response is not included, the optimization cuts the demand power to reduce the power flow in the lines and, consequently, to reduce the voltage drop, which is the main objective of the problem. When the demand response variables are included in the objective function, they are multiplied by a factor (β L) to penalize the use of demand response and the increase of objective function.

A. Inverter control

A cascade control in the dq-frame is proposed. It consists of outer voltage loop and inner current loop [10], [11]. Synchronization with the grid voltage is performed through a phase locked loop (PLL) [12]. The proposed control methodology is depicted in Fig. 5. The d-axis outer loop controls the DC bus voltage, and the inner loop controls the active AC current. Because the inverter allows bidirectional power flow, increments in the DC bus voltage can be produced from negative or positive current direction and vice versa. The q-axis outer loop regulates the AC voltage magnitude by adjusting the reactive current, which is controlled by the q-axis inner current loop. Additionally, dq decoupling-terms ωLinv and feed-forward voltage signals are added to improve the performance during transients.

Fig. 6 shows the PLL block diagram where the input is the measured three-phase voltage at PCC. The output signals vd, θgrid, and ω are obtained to use in the dq-frame inverter control.

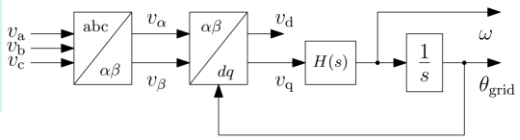

Fig. 6. Charging station PLL block diagram.

Battery charger control

Two equivalent control methodologies can be implemented depending on desired charging strategy: constant current and constant voltage.

Proposed diagram

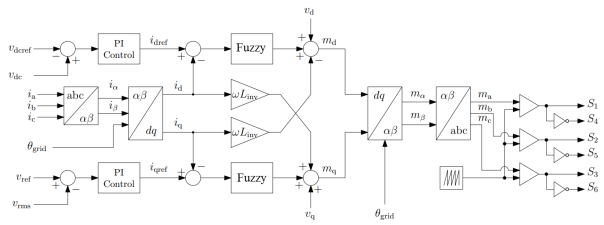

Proposed Charging station control system.

Fig. 7. Battery charger control: (a) constant current strategy, (b) constant voltage strategy.

1) Constant current strategy: It is a unified control strategy equivalent to operating the battery as a current source. The output duty ratio mcc defines the boost-mode operation of the converter. This strategy is depicted in Fig. 7(a).

2) Constant voltage strategy: Analog to the constant current strategy, constant voltage strategy is equivalent to operating the battery as voltage source. The output duty ratio mcv defines the buck-mode operation of the converter. This strategy is depicted in Fig. 7(b).

FUZZY CONTROLLER

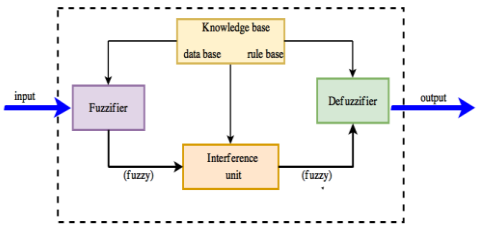

Fig4. Fuzzy controlling block

In the fig4. fuzzy controlling block is shown there the fuzzifier and the defuzzifier functioning blocks are shown. the fuzzy controller is rule based controller. In the Mamdani block the inputs and the outputs are complied and there data base and rule base decision-making unit executes in the Mamdani Block. the fuzzified inputs of FIS and distributes the fuzzy results to defuzzifier, that which gives the outputs of FIS. Finally, the results of all rules are combined and defuzzified.

A. Fuzzification:

In this fuzzification process input values are transformed to fuzzy values. in this the membership functions are based on the linguistic variables is carried out. the fuzzy block contains the preliminary data that are obtain by

- Analog/digital converters with conversion of measured variables.
- The measured variables in order to control the state error integral, state, error derivation and state error of variables.
- Alternative of membership functions for input and output variables that is the number, shape and distribution.

B. Inference:

The decision making part presents, inference operations on fuzzy rules. The fuzzy values within fuzzy rule are aggregated with connective operators like intersection(AND), union (OR) & complement (NOT).

Intersection: $\mathrm{AND}(\mu_a, \mu_b) = \min\{\mu_a, \mu_b\}$ (23)

Union: $\mathrm{OR}(\mu_a, \mu_b) = \max\{\mu_a, \mu_b\}$ (24)

Complement: $\mathrm{NOT}(\mu_a) = 1 - \mu_a$ (25)

where μ_a, and μ_b are membership values, that which are combined by commands. Firing strengths of fuzzy rules are calculated by employing the above commands.

C. Defuzzification:

In defuzzification process, outputs of fuzzy rules are combined to crisp output value. The most common defuzzification strategy is center of the area (COA) [44],

$$Z = \frac{\sum_{i=0}^{n} \mu_i z_i}{\sum_{i=0}^{n} \mu_i} \quad (26)$$

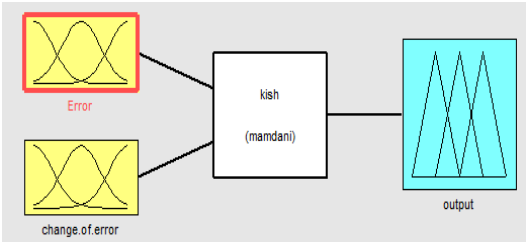

Fig5. shows the fuzzy based Mamadani block with the two inputs error and the change of error and defuziffication output.

The definition of the fuzzy goals and constraints must be defined with developer. consequently, when fuzzy control is measured, tuning strategy can be obtained that it is able to push system closer to constraints, and that is able to force the system to a better performance based on the goals and constraints set by developer. Hence by using dependency between different system variables the fuzzy logic controller can be utilized to calculate weighting factors, the control objectives appropriately and rather than using static values.

SIMULATION RESULTS

Considering the design procedure of the previous Sections, an example model is implemented in Matlab/Simulink SimPower System. Table I gives the input parameters, while Table II gives the resulting parameters of the model. The battery model can be implemented as depicted in Fig. 2 or, alternatively, to use the “battery” block provided in the SimPower Systems Library [13]. The battery charger can be implemented with parameters from Table II and Fig. 3. The inverter can be implemented with the block “universal bridge” from the SimPower Systems Library. It has to be selected “3 arms” and Ron = 0.01 Ω. The transformer can be implemented directly with the “three-phase two windings transformer” block. Finally, the AC source can be implemented with the block “Three-phase source” and the parameters from Table I. The complete model implemented in MATLAB/Simulink SimPower Systems is depicted in Fig. 8, where only two EVs appear as example. Before running the simulation, it is important to set an appropriate simulation time step and an integration method. To achieve good results, the integration method should have at least 100 sample points in a period of the fastest frequency [14]. In the example model, the fastest frequency is fsw = 5000 Hz. The selected integration method is ode23t, and the simulation time step is set as in (9):

Performance to load changes Fig. 9 shows the results of the charging station for a simultaneous connection of two EVs. At t = 0 s, the charging station is operating at no load. At t = 0.2 s, two EVs are simultaneously connected and charged at maximum power as Fig. 9(a) shows. It can be seen that Q is almost not affected by the load change of P from 0 kW to -180 kW. Fig. 9(b) shows the response of the DC bus voltage to this load change. Here, the variation of the voltage is less than 25 V, and it is stabilized in less than 0.1 s.

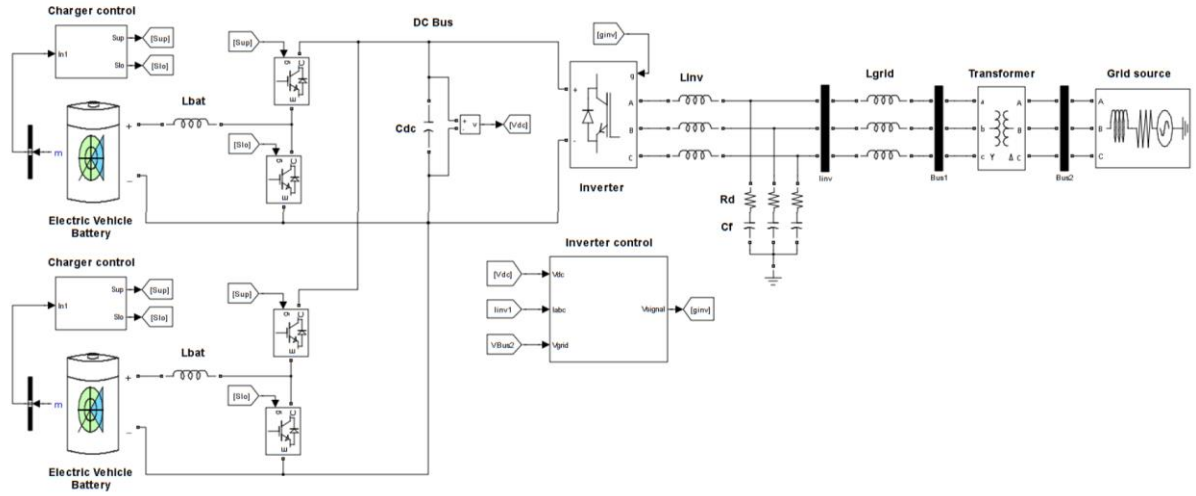

Fig. 8. Matlab/Simulink SimPower Systems implementation of the EV charging station.

Performance to load changes

Fig. 9 shows the results of the charging station for a simultaneous connection of two EVs. At t = 0 s, the charging station is operating at no load. At t = 0.2 s, two EVs are simultaneously connected and charged at maximum power as Fig. 9(a) shows. It can be seen that Q is almost not affected by the load change of P from 0 kW to -180 kW. Fig. 9(b) shows the response of the DC bus voltage to this load change. Here, the variation of the voltage is less than 25 V, and it is stabilized in less than 0.1 s.

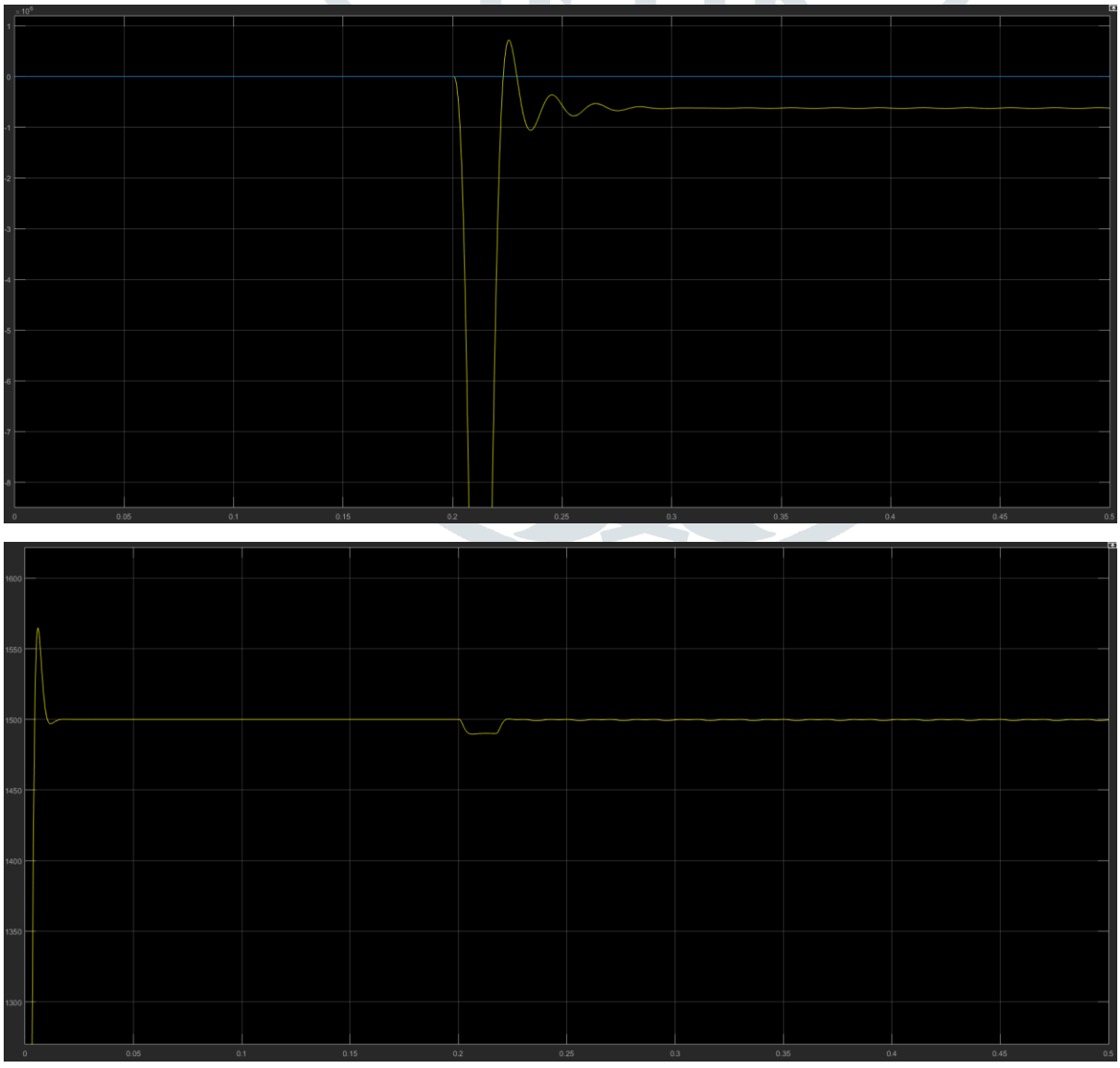

Fig. 9. Charging station results for two EVs load change: (a) active and reactive power, (b) DC bus voltage.

V2G capability and reactive power compensation

Fig. 10 shows the results of the charging station performing V2G and reactive power compensation. Fig. 10(a) shows that at t = 0 s, the charging station is operating at P = −900 kW and Q = 0 kVAr. At t = 0.2 s, V2G at maximum available power and an injection of 150 kVAr are required. Fig. 10(b) shows the response of the DC bus voltage to V2G and reactive power compensation. The change in the current direction influences a positive voltage variation, as it is expected. These results are according to the design parameters for the DC bus capacitance. In addition, reactive power compensation does not affect considerably the dynamics of the DC bus voltage.

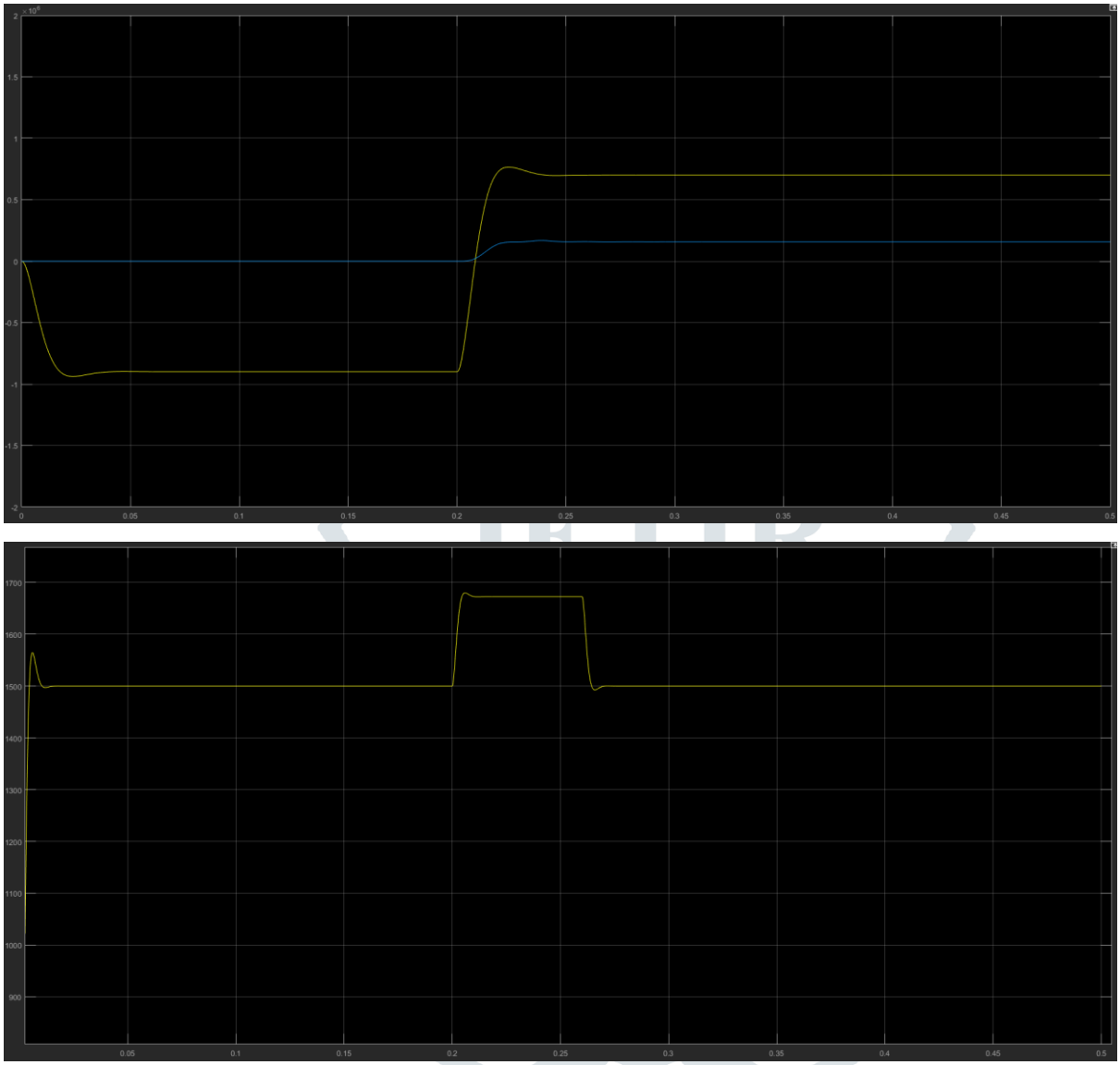

Fig. 10. Charging station results for V2G and reactive power compensation: (a) active and reactive power, (b) DC bus voltage.

Charging and discharging of an EV battery

Fig. 11 shows the results for an EV battery during charging and discharging. The control methodology implemented is constant current. When the battery is charging at constant current, the voltage is higher than its open circuit value as Fig. 11(a) and Fig. 11(b) show, respectively. At t = 0.2 s, the battery is discharged at constant current and the voltage decreases as Fig. 11(a) and Fig. 11(b) demonstrate, respectively. From these results, it can be noticed that, due to the voltage difference, EV charging and V2G have different power rates for the same current.

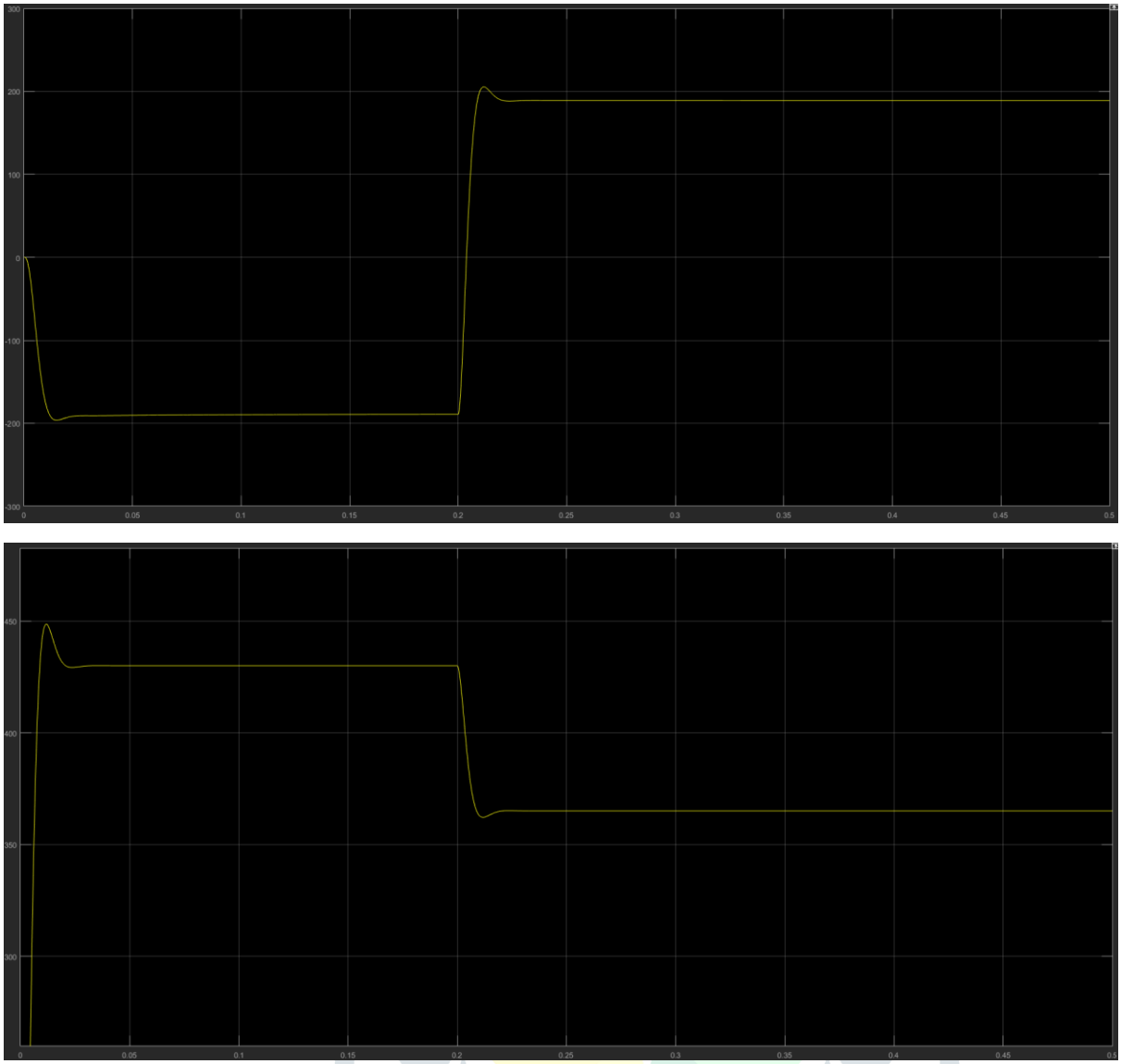

Fig. 11. Individual EV battery results for charging and discharging: (a) battery voltage, (b) battery current.

CONCLUSIONS

A new model of a charging station for fast DC charging is presented. The modeling of every component is presented with their corresponding parameters. In addition, a control system is also included. It can be concluded that the most appropriate strategy in each case depends on the objective sought: Regarding power quality, by using DSC control strategy for active control, better results are attained, since the charger current has a very small THD. However, if what is looked for is to reduce the RMS charger current to minimize power losses, the RB strategy achieves better results with a higher PF value. he voltage restored reaches the original stator voltage as soon as DVR or the V2G system is switched on. The voltage across the DC link capacitor falls to a low value without any compensation which is also brought to its original value with the compensation. The results showed clearly that employing fuzzy control for both supplementary devices yields a better control than a PI controller. Simulation tests have been conducted charging and discharging the battery from the grid using different control strategies and set-points sent by the aggregator. These results validate the proper operation of the control stage of the battery charger. A charging station model was also designed to support V2G and reactive power compensation. Simulation results show a proper dynamic behavior of the DC bus voltage, the battery voltage, and the battery current. Moreover, the results show that a smooth transition to V2G and reactive power compensation are possible.

REFERENCES

[1] http://www.sae.org/smartgrid/chargingspeeds.pdf

[2] Karlsson, P. Svensson, J. , ”DC bus voltage control for a distributed power system,” Power Electronics, IEEE Transactions on , vol.18, no.6, pp. 1405- 1412, Nov. 2003.

[3] Mishra, M.K. Karthikeyan, K. , ”A Fast-Acting DC-Link Voltage Controller for Three-Phase DSTATCOM to Compensate AC and DC Loads,” Power Delivery, IEEE Transactions on , vol.24, no.4, pp.2291-2299, Oct. 2009.

[4] Min Chen and Rincon-Mora, G.A., ”Accurate electrical battery model capable of predicting runtime and I-V performance” IEEE Transactions on Energy Conversion, VOL. 21, NO. 2, June 2006.

[5] Mohan, N. ”First Course on Power Electronics Converters and Drives” Minneapolis, USA. ISBN 0-9715292-2-1.

[6] Dannehl, J. Fuchs, F.W. Thgersen, P.B. , "PI State Space Current Control of Grid-Connected PWM Converters With LCL Filters," Power Electronics, IEEE Transactions on , vol.25, no.9, pp.2320-2330, Sept. 2010.

[7] Min-Young Park, Min-Hun Chi, Jong-Hyoung Park, Heung-Geun Kim, Tae-Won Chun, Em-Cheol Nho, "LCL-filter design for grid-connected PCS using total harmonic distortion and ripple attenuation factor," Power Electronics Conference (IPEC), 2010 International , vol., no., pp.1688-1694, 21-24 June 2010.

[8] Araujo, S.V. Engler, A. Sahan, B. Antunes, F., "LCL filter design for gridconnected NPC inverters in offshore wind turbines," Power Electronics, 2007. ICPE '07. 7th Internatonal Conference on , vol., no., pp.1133-1138, 22-26 Oct. 2007.

[9] M. Tavakolini Bina, E. Pashajavid "An efficient procedure to design passive LCL-filters for active power filters"'. Electric System Power Research. 2009.

[10] Yazdani, A. Iravani, R. "Voltage-Sourced Converters in Power Systems - Modeling, Control and Applications" John Wiley and Sons, 2009 - Technology and Engineering.

[11] Blaabjerg, F. Teodorescu, R. Liserre, M. Timbus, A.V., "Overview of Control and Grid Synchronization for Distributed Power Generation Systems," Industrial Electronics, IEEE Transactions on , vol.53, no.5, pp.1398-1409, Oct. 2006.

[12] Se-Kyo Chung, "A phase tracking system for three phase utility interface inverters ," Power Electronics, IEEE Transactions on , vol.15, no.3, pp.431-438, May 2000.

[13] MATLAB Simulink SimPowerSystems 7.6 (R2008a) "SimPowerSystems Library Documentation" 2008.

[14] Mohan, N. Undeland, T. Robbins, W. "Power Electronics Converters, Applications, and Design" ISBN 0-471-22693-9.

AUTHORS DETAILS

Ms. J LATHA received a Diploma in Electrical and Electronics Engineering from Government polytechnic college, Kotagiri, Nizambad(Dist), Telangana, India. And received a B.Tech Degree in EEE from Vijay Rural Engineering College, Nizambad(Dist), Telangana, India from JNT University. And studying M.tech in Electrical Power System at Holy Mary Institute of Technology and Science, Bogaram (V), Medchal (Dist), Hyderabad, in the Dept. of Electrical & Electronics Engineering.

Dr. G. Jayakrishna has received his B.Tech degree in Electrical and Electronics Engineering and M.Tech in Electrical Power Systems from JNTU, Hyderabad, and Ph.D. Degree in Electrical Engineering from JNTUA, Anantapur, Andhra Pradesh, India. Presently he is working as a Professor in the Department of Electrical and Electronics Engineering, Holy Mary Institute of Technology and Science, Hyderabad, Telangana. He is having 25 years of teaching experience. His research interests include Power quality improvement, AI Techniques and renewable energy sources.